JOURNAL OF MATERIALS SCIENCE 35 (2000) 2361–2369

The abrasive corrosion behavior of plasma-nitrided alloy steels in chloride environments

C. K. LEE‡, H. C. SHIH*
Department of Materials Science and Engineering, National Tsing Hua University, Hsinchu, Taiwan 300, ROC
E-mail: hcshih@mse.nthu.edu.tw

Both corrosion and abrasive corrosion behavior of plama-nitrided type 304 and 410 stainless steels and 4140 low alloy steel were investigated in 3% NaCl solution (pH = 6.8) by electrochemical corrosion measurements. Surface morphology and alloying elements after corrosion and abrasion corrosion tests were examined by scanning electron microscopy and energy dispersive analysis of X-rays. The results indicated that the plasma-nitrided SAE 4140 steel containing ε-$(Fe,Cr)_{2-3}N$ and γ'-$(Fe,Cr)_4N$ surface nitrides which produce a thick and dense protective layer exhibited a significant decrease of corrosion currents by inhibition of the anodic dissolution of iron, whereas the plasma-nitrided type 304 and 410 stainless steels containing the segregation of chromium nitride CrN exhibited an extensive pitting corrosion by acceleration of the anodic dissolution of iron. It is concluded that the susceptibility to pitting is consistent with the degree of chromium segregation, and decreases as follows: 304 stainless steel > 410 stainless steel > 4140 steel. Also, the results of abrasive corrosion testing for the plasma-nitrided alloys are strongly related to the subtleties of the nitrided microstructures resulting in a pitting and spalling type of abrasive corrosion of type 304 and 410 stainless steels, and excellent abrasive corrosion resistance for SAE 4140 steel.

1. Introduction

During the last decade, plasma thermochemical heat treatment techniques have been developed [1, 2], and are now extensively used by industry for the nitriding of steels to improve their mechanical properties, such as wear and fatigue resistance. Ion-implantation method has also shown the potential for improving wear properties [3–5]. Among several species, nitrogen has been used extensively because it combines the economic advantages of a gaseous source with a well-established efficacy for hardening metals [5]. Although both techniques can improve the mechanical properties of steels, these treatments also affect the oxidation and corrosion resistance of materials. Depending on the type of material and environment, nitriding may improve or deteriorate the corrosion resistance of steels. A beneficial effect of nitriding on corrosion for low alloy steels in some aqueous solutions has been claimed by some investigators [6–8].

It is well known that nitrogen as an alloying element has a beneficial effect on the passivation and pitting resistance for austenitic stainless steels [9–13]. Because nitrogen exists in the form of solid solution for N-contained alloy or in the form of nitrides for N-implanted metal and nitrided metal; the corrosion behaviors for various N-systems should be quite different. Despite considerable recent efforts expended in investigating the corrosion behaviors of N-contained alloys [14, 15], including the present authors [16, 17], and some studies concerning N-implantation have initiated [18, 19]. However, further detailed study concerning the relationship between chemical composition, structure and electrochemical properties for plasma- nitrided steels are still needed. Moreover, few studies have dealt with the abrasive corrosion resistance of plasma-nitrided steels.

The aim of the present study was to examine both the corrosion and abrasive corrosion characteristics of the three plasma-nitrided ferrous materials including SAE 304 and 410 stainless steels and 4140 low alloy steels in 3% NaCl solution. It was hoped to correlate the experimental electrochemical data for plasma-nitrided steels with the structure of the nitrided layer and to demonstrate it mechanistically.

‡ *Present Address*: Department of Mechanical Engineering, Chien Hsin Institute of Technology, Chungli, Taiwan 320, ROC.

* Author to whom all correspondence should be addressed.

2. Experimental

2.1. Sample preparation

Commercial SAE 304 and 410 stainless steels and SAE 4140 low alloy steel were employed as the test materials. Elemental analyses of the various alloys are given in Table I. As-received 304 stainless steel was homogenized at 1050 °C for 1 hour, then quenched in water. The 410 stainless steel was first preheated at 760 °C for 7 min. because of its lower thermal conductivity, then heated to the annealing temperature of 960 °C for 1 hour, quenched in rapidly circulating air, and followed by tempering at 600 °C for 2 hours. SAE 4140 steel was annealed at 840 °C for 1 hour, quenched in oil, tempered at 650 °C for 2 hours, then cooled in air. After heat treating, the steels were machined to hollow cylindrical (ring) specimens (inside diameter 14 mm; outside diameter 23 mm; width 16 mm). Before plasma nitriding, all specimens were ground with emery papers up to 1200 grit and cleaned with acetone in an ultrasonic cleaner.

The nitriding process was performed as follows: (1) As soon as specimens were put into the nitriding chamber, the chamber was evacuated to 1.0×10^{-2} Torr, (2) 0.5 Torr of an argon-hydrogen mixture (argon to hydrogen ratio, 1 : 1) was allowed to flow into the chamber, and the specimens were heated by plasma. As soon as the temperature reached 560 °C, the gas mixture was replaced with a nitrogen-hydrogen mixture (nitrogen to hydrogen ratio, 2 : 1) having a total pressure of 3 Torr. The nitriding was subsequently performed in the plasma at 560 °C for 50 hours, (3) Before the specimens were removed from the vacuum chamber, they were cooled below 150 °C.

2.2. Microstructure analysis

X-ray diffraction (XRD) was used to identify the phases formed in the nitrided zone. Cu K_α radiation was used in all these analyses. Optical microscopy was employed to examine the cross-section of the plasma nitrided layers.

2.3. Electrochemical corrosion and abrasive corrosion test

The corrosion behavior of all specimens before and after nitriding was studied by potentiodynamic polarization tests. All potentials were measured against a saturated calomel electrode (S.C.E.). Samples were pretreated cathodically at −1200 mV (S.C.E.) for 2 min. Thereafter, potentiodynamic scanning at a rate of 1 mV/s, was conducted from cathodic toward anodic direction up to +1200 mV (S.C.E.). The corrosion morphology was examined by scannning electron microscopy (SEM) and energy-dispersive spectroscopy (EDS) was applied for composition analyses.

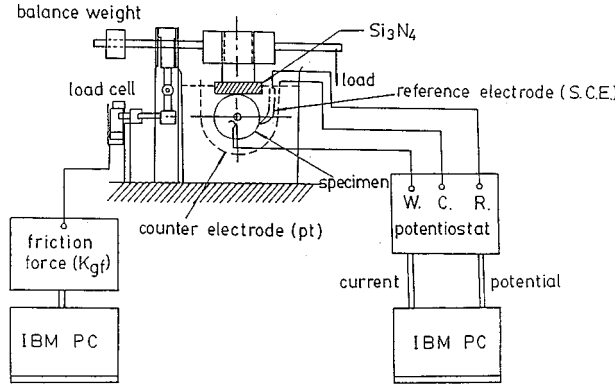

Figure 1 Electrochemical abrasive corrosion testing apparatus.

The abrasive corrosion behavior of plasma nitrided specimens were evaluated by performing cyclic potentiodynamic ploarization during abrasion. The same scanning rate of 1 mV/s was applied in the noble direction from −1200 mV (S.C.E.) to +400 mV (S.C.E.) or until the current density just exceeded $10^3 \mu A/cm^2$, whichever came first, and then scanned reversely to −1200 mV (S.C.E.). A block-on-ring abrasive corrosion testing apparatus, as shown in Fig. 1, was used to measure the friction coefficient, μ and electrochemical characteristics. The tests were conducted by pressing a sintered Si_3N_4 (surface hardness, ∼1455 Hv) block against the center edge of ring nitrided specimen, under the abrading conditions of 1.12 Kgf and 200 rev./min. The friction force at the contact area was recorded through the load cell and, with the help of an IBM personal computer, was recorded and automatically divided by the applied load (N) to obtain the friction coefficient ($\mu = F/N$). A PARC Model 273 potentiostat/galvanostat was used, and also interfaced with an IBM personal computer.

3. Results and discussion

3.1. Microstructure of plasma nitrided samples

3.1.1. Microhardness measurements

Three distinct microhardness depth profiles of plasma nitrided type 304 stainless steel, 410 stainless steel and SAE 4140 steel are shown in Fig. 2. It is clearly shown that the nitrided layer on 4140 steel (∼0.2 mm) is almost twice the thickness of that on 304 stainless steel or 410 stainless steel (∼0.1 mm). As far as the magnitude of the surface hardness, the steels can be arranged as follows: 4140 steel (1275 Hv) > 410 stainless steel (1132 Hv) > 304 stainless steel (1016 Hv). This result is comparable with earlier reports [1, 20, 21].

TABLE I Chemical composition (wt%) of the alloys

	Element amount (wt%)									
Materials	C	Si	Mn	P	S	Mo	Cu	Ni	Cr	Fe
SAE 304	0.038	0.61	1.46	0.026	0.007	—	—	8.38	17.70	Bal.
SAE 410	0.151	0.653	0.305	0.035	0.004	—	—	—	11.63	Bal.
SAE 4140	0.45	0.27	0.71	0.014	0.004	0.23	0.015	0.023	1.01	Bal.

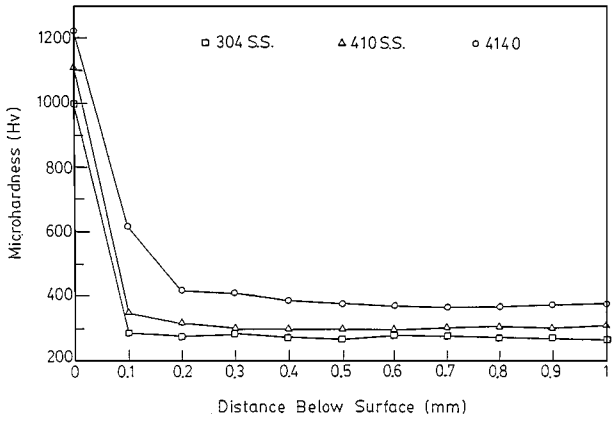

Figure 2 Microhardness depth profiles of plasms-nitrided steels (nitriding temperature, 560 °C; treatment time 50 h; load for hardness measurement, 500 gf).

3.1.2. Analysis of nitrided layers

Photomicrographs of the cross-sections of the plasma nitrided alloys are shown in Fig. 3. The phases formed in the nitrided layers were identified by XRD as shown in Fig. 4. It can be seen that the nitrided surface layer of SAE 4140 steel consists primarily of a mixture of γ'-$(Fe,Cr)_4N$ and ε-$(Fe,Cr)_{2-3}N$ phases. However, the nitrided surface on type 304 stainless steel consists of CrN precipitates and γ-Fe with γ' and ε phases; and, type 410 stainless steel, it consists of CrN precipitate and α-Fe with γ' and ε phases. This result can be explained by the higher chromium content of 304 stainless steel (18 wt % Cr) and 410 stainless steel (12 wt % Cr) and its associated higher affinity for nitrogen; and by the significant solubility ($\sim$5 wt %) of nitrogen in the ε phase [7]. Etching was performed in nital or one of the several alternatives [22]. These experiments supported the existence of a multilayer formation which can be divided into [23–25]:

(i) a compound layer or a "white layer" formed by ε and γ' type phases.

(ii) a diffusion layer of CrN or Cr_2N in the matrix.

In the micrographs shown only 4140 (Fig. 3c) has a clearly observable and distinguishable compound layer and diffusion zone. For the 304 and 410 stainless steels a compound layer cannot be observed. The absence of a compound layer on the stainless steels may be supported by the X-ray diffractograms. A considerable intensity of the ε-nitride peaks is observed only for 4140 steel. It can also explain the higher surface hardness value of the plasma nitrided 4140 steel.

It is also seen that SAE 4140 has a much larger depth of nitrided layer ($\sim$230 μm) than that of type 304 stainless steel ($\sim$100.5 μm) and 410 stainless steel ($\sim$110 μm). This finding is consistent with the microhardness depth profiles reported above. The results are also supported by the explanation that, from a thermodynamic viewpoint, the nitrided layers on both type 304 stainless steel and 410 stainless steel, enriched with CrN precipitates, are thermodynamically more stable than iron nitrides (ε and γ' phases) [22]. In other words, the formation of ε and γ' requires a higher nitrogen potential than is required for chromium nitrides, and thus it lowers the nitrogen diffusion potential resulting in the decreases of the nitrided depth.

3.2. Electrochemical determination of the corrosion and abrasive corrosion properties

For the electrochemical corrosion measurements potentiodynamic polarization tests were performed in 3% NaCl solution to study the pitting tendencies of the samples. Fig. 5 shows the potentiodynamic polarization curves of both untreated and nitrided samples, and the associated characteristic electrochemical data are listed in Table II. It is seen that the corrosion potential ($-$685 mV) of untreated SAE 4140 steel shifts to a noble value ($-$480 mV) after nitriding and the corrosion current density is decreased from 31.6 to 5.8 $\mu A/cm^2$. In contrast, the corrosion potentials of both type 304 stainless steel and 410 stainless steel become more active after nitriding; and the corrosion current for 410 stainless steel increases greatly (from 7.9 to 14 $\mu A/cm^2$) but decrease slightly for 304 stainless steel (from 6.3 to 15 $\mu A/cm^2$). Furthermore, Fig. 5b shows that nitrided SAE 4140 steel has the lowest anodic current density among the three nitrided alloys, although no passivity is apparent. This result indicates that the general corrosion resistance of SAE 4140 steel is improved by nitriding quite significantly. The lack of passivity for nitrided SAE 4140 steel can be explained by its low chromium content (1 wt % Cr) and the high chloride concentration of the solution (3 wt % NaCl).The improvement of passivity for nitrided SAE 4140 steel has been shown in lower chloride solutions (0.1 wt % NaCl), and is supported by a nitrogen dissolution model in which the consumption of acid in pit nuclei occurs by the following reaction [16, 17]:

$$[N] + 4H^+ + 3e \rightarrow NH_4^+ \qquad (1)$$

The reduced anodic dissolution rates in nitrided 4140 can be accounted for by the enrichment of N atoms in a porous nitrided layer, as supported by the previous work [16]. Furthermore, it is noted that nitriding of either type 304 stainless steel or 410 stainless steel causes a significant decrease of the passive potential range, and greatly increases both the passive current density and the critical current density, as shown in Table II. These results demonstrate that nitriding causes both type 304 stainless steel and 410 stainless steel to have rather unstable passivity, which is easily broken down in the presence of chloride ions, leading to pitting or crevice corrosion.

It is of interest to further evaluate the corrosion resistance of the nitrided alloys under abrading conditions. Abrading action can destroy the protective oxide film which is always present on metallic surfaces, or can develop better corrosion-resistant films by producing new surfaces of considerably high chemical reactivity [26]. The cyclic voltammograms during different abrasion conditions have been successfully applied to evaluate effect of anodic film dissolution due to the mechanical wear for low alloy steel in 1% NaCl solution [27].

The results of the cyclic potentiodynamic polarization curves during abrasion for the three plasma nitrided

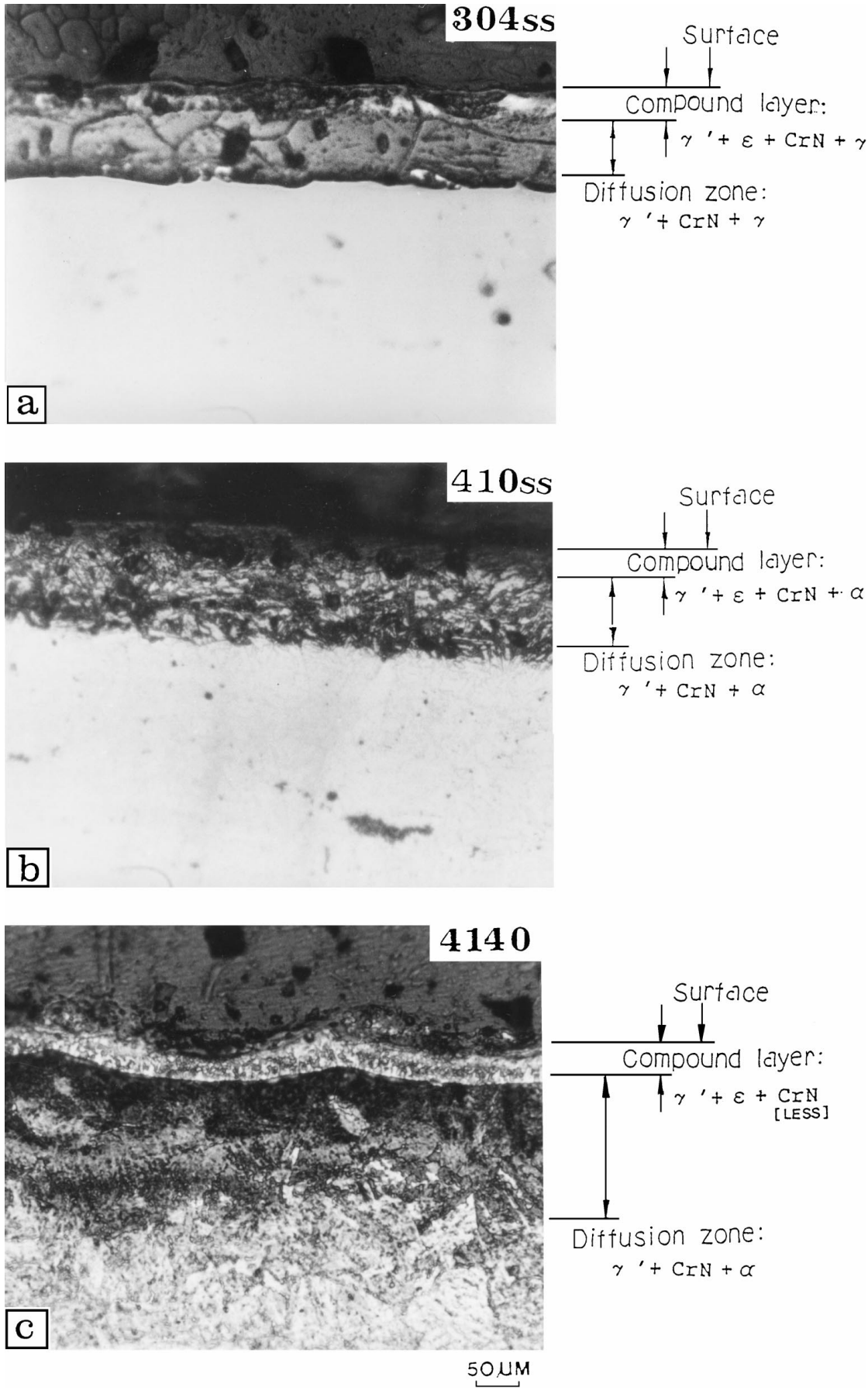

Figure 3 Photomicrographs of the cross sections of the plasma nitrided steels: (a) 304 stainless steel; (b) 410 stainless steel; (c) 4140 steel.

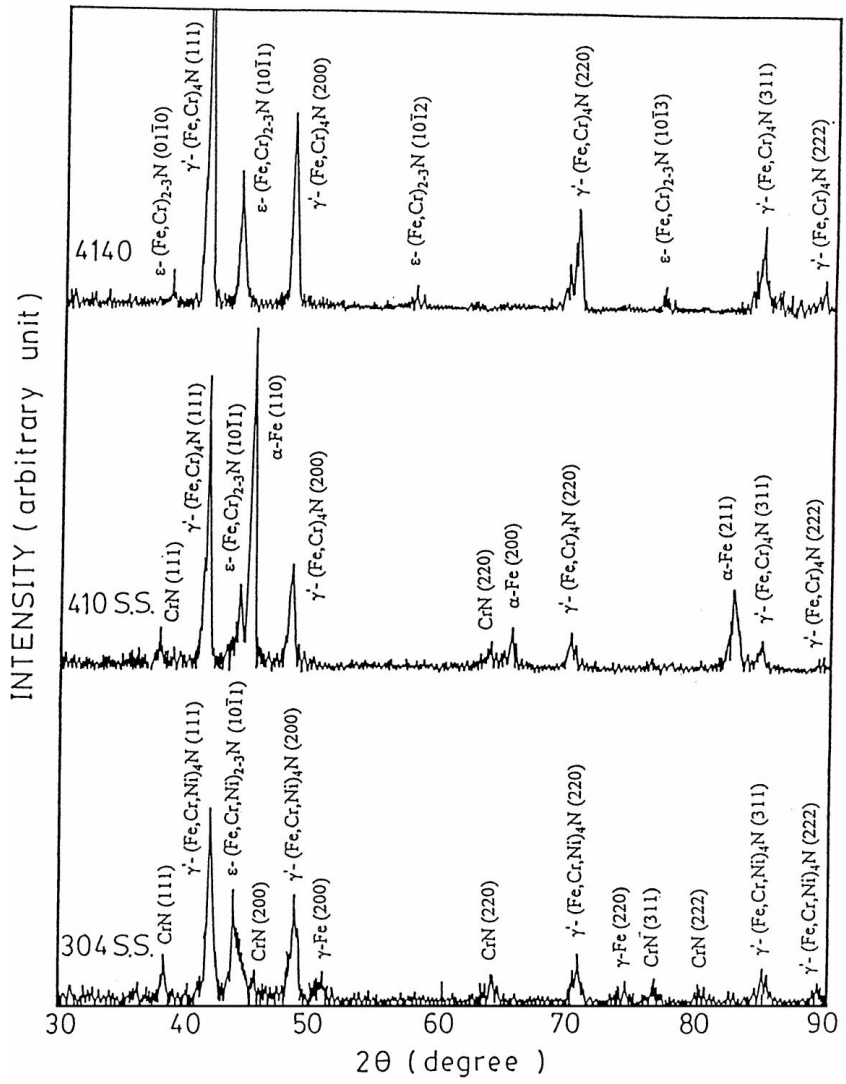

Figure 4 X-ray diffraction patterns for the nitrided alloys.

specimens are shown in Fig. 6. The characteristic values obtained from these polarization curves are listed in Table III. For type 410 stainless steel and SAE 4140 steel the corrosion potential after abrasion has changed to a more noble value by +86 and +295 mV, respectively, and the corresponding corrosion current density has been decreased to -0.2 μA/cm^2 for type 410 stainless steel and -0.6 μA/cm^2 for SAE 4140 steel. On the contrary, type 304 stainless steel shows an increase of the corrosion current density after abrasion ($+1.9$ μA/cm^2) and shifts its corrosion potential to more active potential (-50 mV). It can be concluded that the resistance to abrasive corrosion for these three alloys is arranged as following order: SAE 4140 steel > 410 stainless steel > 304 stainless steel. This result is consistent with the order of the inhomogeneous structures and the stability of passive films in static state for these three alloys as previous microstructural analyses and static potentiodynamic polarization tests. Thus, the inhomogeneous structures for type 304 stainless steel and 410 stainless steel after nitriding may enhance the local corrosion resulting the deterioration of passive film and also reduce the ability to reform the layer for the mechanical abrasion action.

3.3. Microstructural changes due to electrochemical testing

Fig. 7 shows the SEM photomicrographs and EDS analyses of the corroded surfaces of nitrided samples after potentiodynamic polarization tests in 3% NaCl solution. The susceptibility to pitting is consistent with the degree of chromium segregation, with pitting being worst in 304 stainless steel, somewhat less in 410 stainless steel, and the least in 4140 steel. This result is also consistent with the suggestion that CrN is precipitated in the matrix of iron nitrides in SAE 4140 steel.

So far, the results suggest the following mechanism of pitting corrosion in both plasma nitrided 304 stainless steel and 410 stainless steel: γ-Fe (304 stainless steel) and α-Fe (410 stainless steel) are dissolved first; the hydrolysis of the metal ions then increases the acidity of the local solution in the vicinity of the pit site, for example, through the reactions:

$$Fe^{2+} + H_2O \Leftrightarrow FeOH^+ + H^+ \quad (2)$$

$$Fe^{2+} + 2H_2O \Leftrightarrow Fe(OH)_2 + 2H^+ \quad (3)$$

$$2Fe^{3+} + 3H_2O \Leftrightarrow Fe_2O_3 + 6H^+ \quad (4)$$

$$3Fe^{2+} + 2H_2O + O_2 \Leftrightarrow Fe_3O_4 + 4H^+ \quad (5)$$

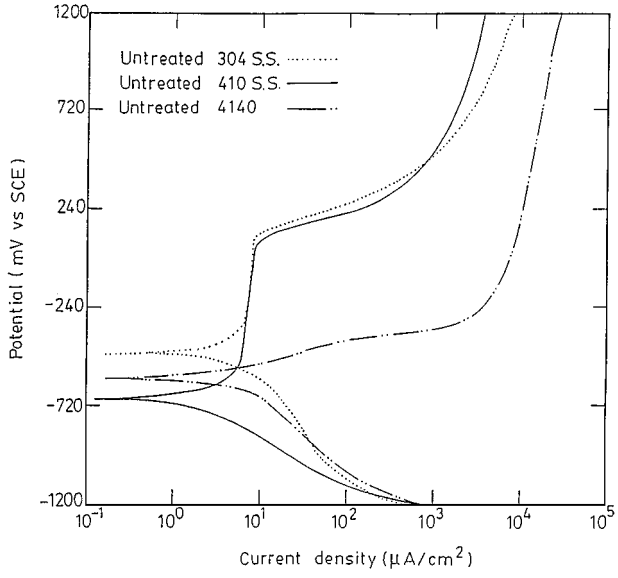

(a)

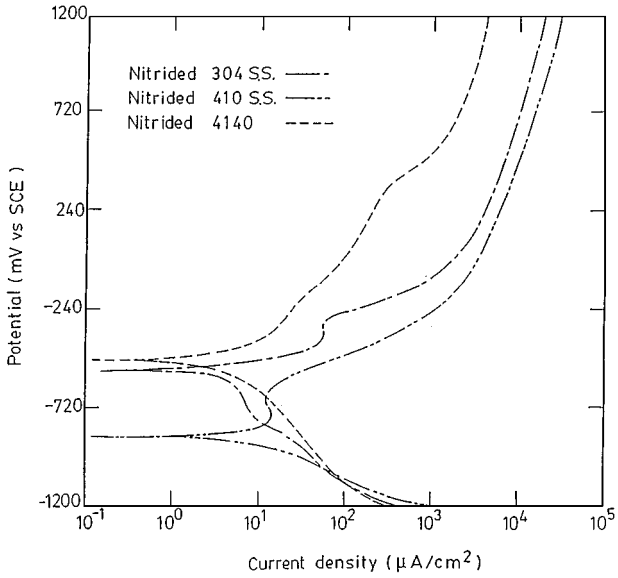

(b)

Figure 5 Potentiodynamic polarization curves for (a) untreated and (b) nitrided steels in 3% NaCl solution (pH = 6.8).

This acidification will autocatalytically accelerate the anodic dissolution at the pit site [28]. Inhomogeneous microstructures enhance corrosion due to electrolytic cell reaction between second phase particles and the matrix, whereas homogeneous structures are relatively free of internal cell reactions [29]. Therefore, when the large amounts of CrN precipitates result in substantial chromium segregation in 304 and 410 stainless steels, local galvanic cells will be set up which further enhances the pitting corrosion. In contrast, Fig. 7c reveals only shallow pits in nitrided SAE 4140 steel whose black regions showing evidence of dissolved nitrogen. This significant finding can be explained by the enrichment of Cr and N building up within the porous channels of nitrided layer. This suggestion is comparable with the model suggested by Newman and his coworkers [13, 30], that nitrogen atoms enrich the active sites and dissolve in preference to metal elements. Furthermore, a higher nitrogen content (about 7%) has a neutralizing effect in acid pits [17].

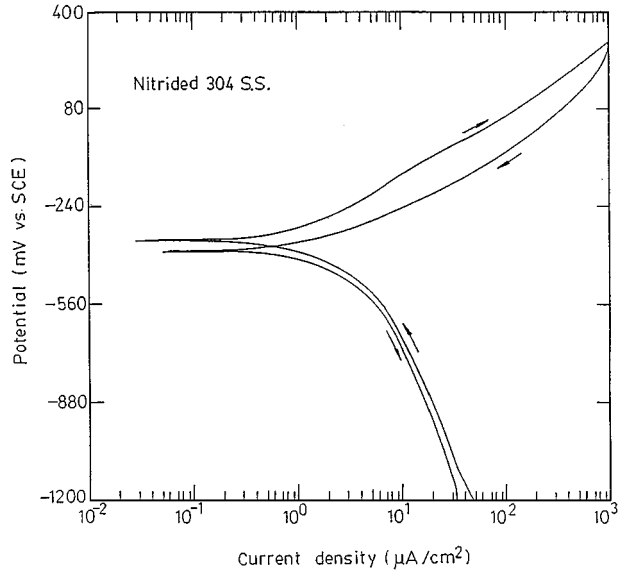

(a)

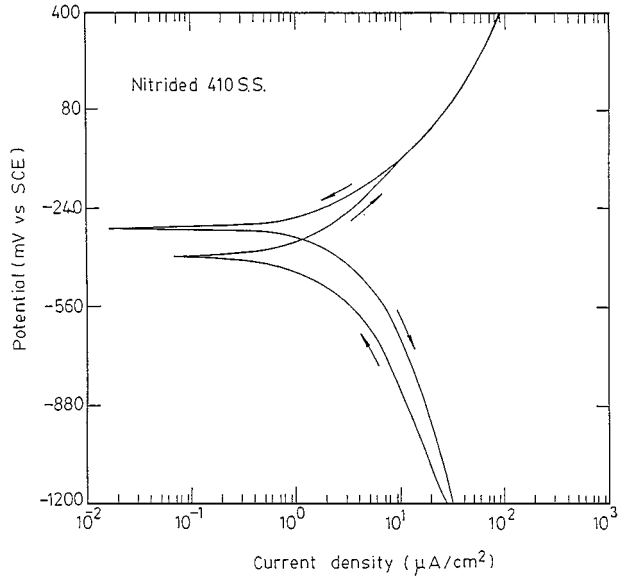

(b)

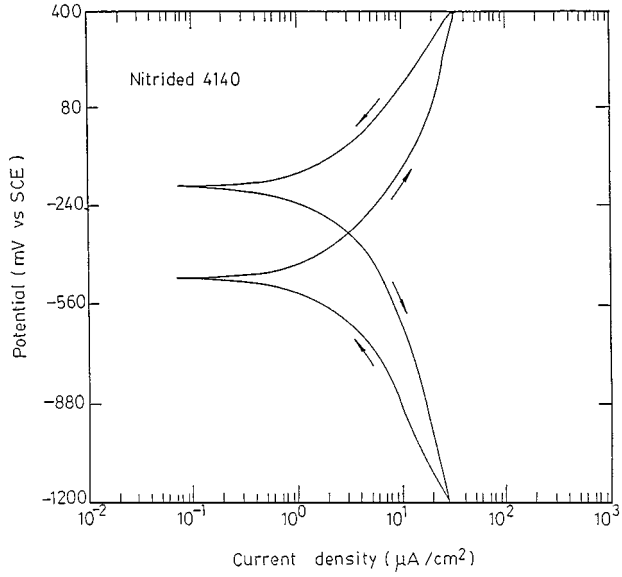

(c)

Figure 6 Cyclic potentiodynamic polarization curves during abrasion for the plasma nitrided specimens: (a) 304 stainless steel; (b) 410 stainless steel; (c) 4140 steel.

TABLE II Characteristic electrochemical data from potentiodynamic polarization curves

	ϕ_{corr} (mV)		ϕ_b (mV)		ϕ_p (mV)		$\Delta\phi_p$ (mV)		i_{corr} (μA/cm^2)		i_p (μA/cm^2)		i_{crit} (μA/cm^2)	
Alloys	U	N	U	N	U	N	U	N	U	N	U	N	U	N
304	−478	−549	102	−309	−326	−415	428	106	6.3	15.1	8	63	8	64
410	−582	−857	60	−634	−513	−772	573	138	7.9	14	7	15	7	16
4140	−685	−480	—	—	—	—	—	—	31.6	5.8	—	—	—	—

U-untreated.
N-nitrided.

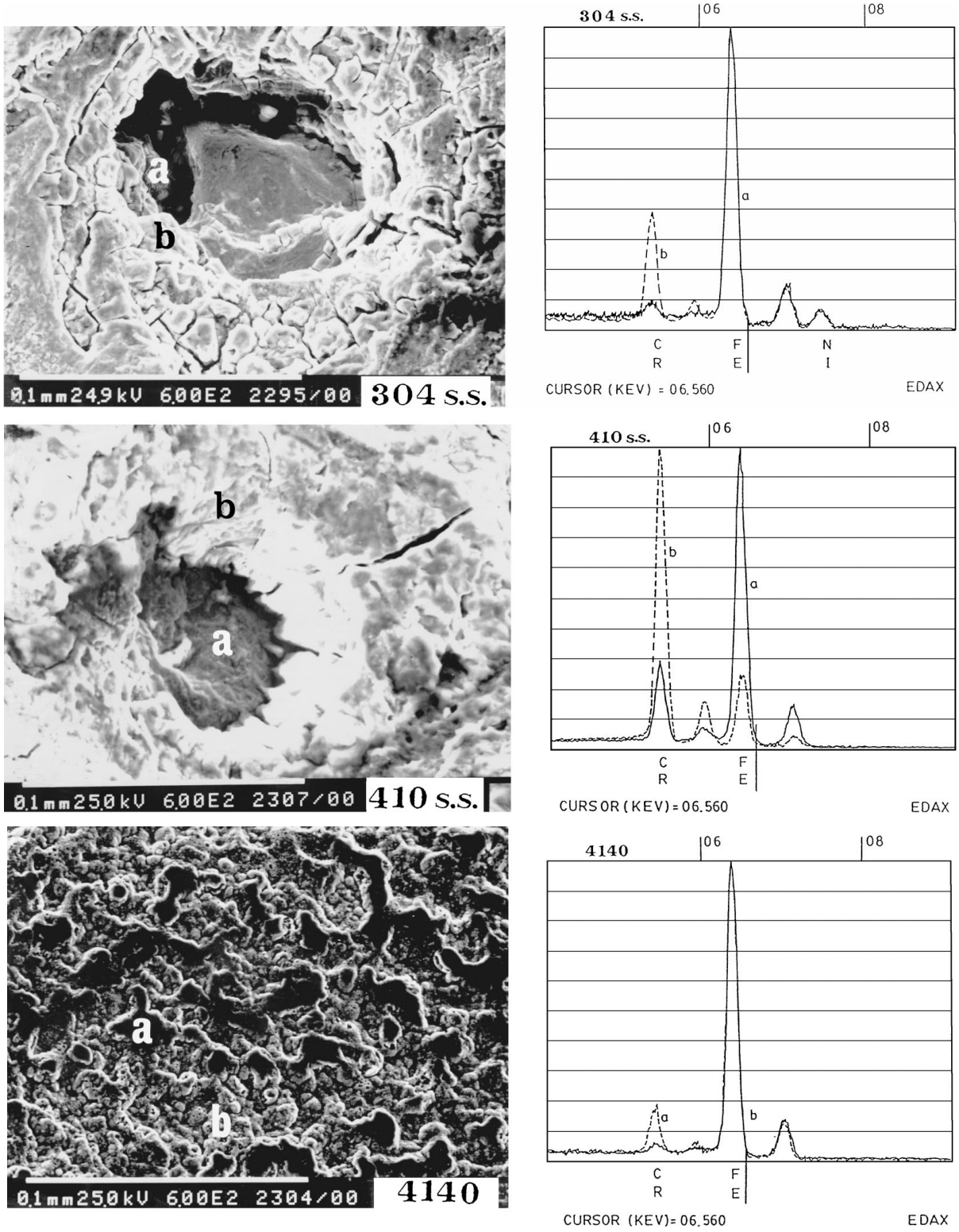

Figure 7 SEM images and EDS analyses of the corroded nitrided steels after the electrochemical corrosion test.

TABLE III Characteristic electrochemical data from cyclic potentiodynamic polarization curves during abrasion for nitrided steels

Alloys	ϕ_{corr} (mV) Before	ϕ_{corr} (mV) After	$\Delta\phi_{corr}$ (mV)	i_{corr} (μA/cm^2) Before	i_{corr} (μA/cm^2) After	Δi_{corr} (μA/cm^2)
304	−338	−388	−50	1.5	3.4	+1.9
410	−395	−309	+86	1.7	1.5	−0.2
4140	−466	−171	+295	2.6	2.0	−0.6

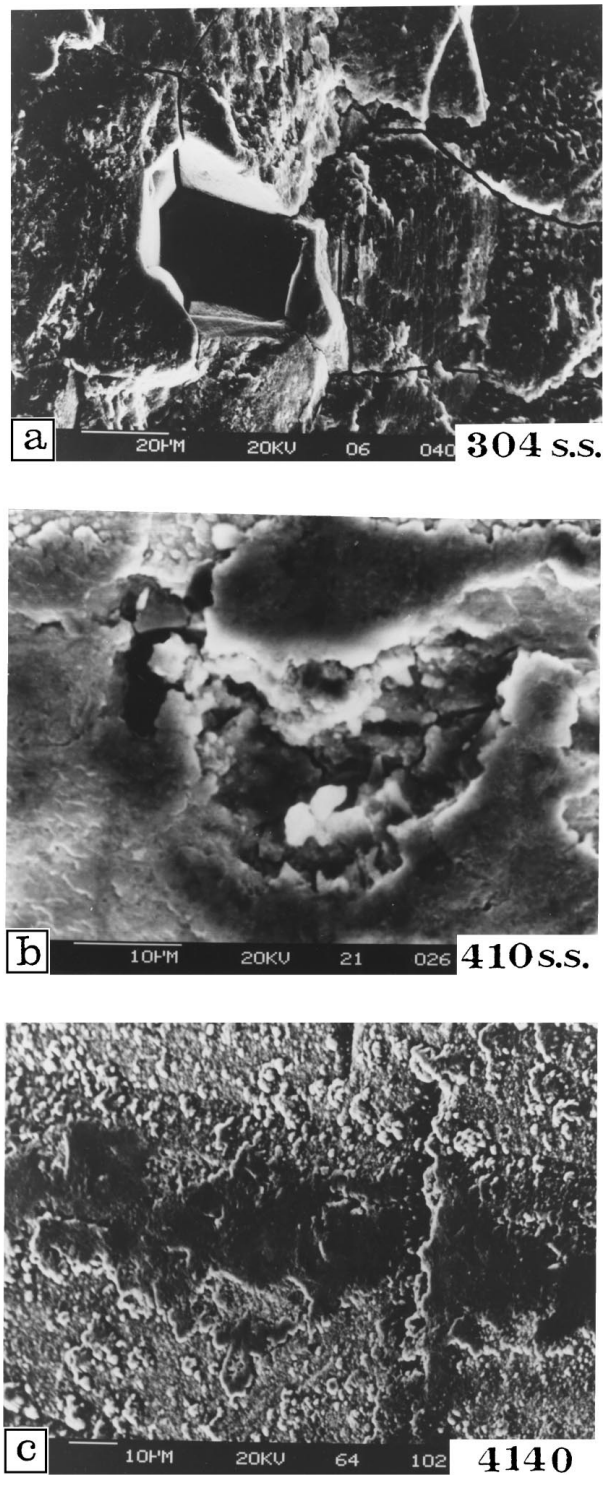

Figure 8 The morphology of abrasion scars after cyclic potentiodynamic polarization test during abrasion for the plasma nitrided specimens: (a) 304 stainless steel; (b) 410 stainless steel; (c) 4140 steel.

Fig. 8 shows the morphology of abrasion scars after cyclic potentiodynamic polarization test during abrasion for the plasma-nitrided specimens. It is seen that the surface of the nitrided 304 stainless steel contains obviously intergranular cracks. Furthermore, nitrided 410 stainless steel not only exhibits cracking in the nitrided layer but also in the substrate below. In contrast, nitrided SAE 4140 steel shows the smooth abrasion scar without any cracks. Thus, the abrasive corrosion mechanism can be categorized as a pitting and spalling type of wear, which is due to the formation and removal of chemical reaction films [31–33]. However, SAE 4140 steel has a nitrided layer with a homogeneous structure ($\varepsilon + \gamma'$ phases) enriched with Cr and N atoms. This type of microstructure increases the pitting resistance and produces good film lubrication without any abrasive corrosion fracture, because nitrogen is dissolved preferentially (the black scars shown in Fig. 8c).This consideration is in fact consistent with the friction coefficient, μ, resulting from the abrasive corrosion test and the order of the μ value can be arranged as follows: 304 stainless steel ($\sim$0.112) > 410 stainless steel ($\sim$0.090) > SAE 4140 steel ($\sim$0.074).

4. Summary and conclusions

(1) The depth of the nitriding layer on SAE 4140 steel ($\sim$230 μm) is almost twice the thickness of that on type 304 stainless steel ($\sim$100.5 μm) and 410 stainless steel ($\sim$110 μm). The alloys may be listed in order of decreasing surface hardness as follows: SAE 4140 steel (1275 Hv) > 410 stainless steel (1132 Hv) > 304 stainless steel (1016 Hv).

(2) Plasma nitrided 4140 steel shows better corrosion and abrasive corrosion properties than plasma nitrided 304 and 410 stainless steels due to the presence of an isolating compound layer at the surface. The stainless steels are not covered by a compound layer, but due to the large amount of Cr in these alloys, which consumes all nitrogen supplied so nothing is left for the nucleation and growth of an iron nitrided layer, only a diffusion zone has formed during nitriding (which contains a dispersion of Cr- and Fe-nitrides). The latter heterogeneous structure promotes corrosive attack.

(3) The pitting and spalling type of wear mechanism may be responsible for the abrasive corrosion of both nitrided 304 and 410 stainless steels.

References

1. "Metals Handbook, Vol.4," 9th ed. (American Society for Metals, Metals Park, OH, 1981) p. 191.
2. B. EDENHOFER, *Heat Treat. Met.* **1** (1974) 23 and 59.
3. H. HONG, R. F. HOCHMAN and T. F. J. QUINN, "Surface Modifications and Coatings," (ASM, Metals Park, Ohio, 1986) p. 455.
4. H. HONG, W. B. CARTER and R. F. HOCHMAN, *Corrosion* **44** (1988) 611.
5. W. C. OLIVER, R. HUTCHINGS and J. B. PETHIA, *Met. Trans. A* **15** (1985) 2221.
6. V. G. REVENKO, G. P. CHERNOVA and V. V. PARSHUTIN, *Zashchita Metallov* **24** (1988), 204.
7. K. IBENDORF and W. SCHROTER, *Surf. Eng.* **4** (1988) 327.

8. L. FEDRIZZI, L. GUZMAN, E. MIGLIO, G. CERISOLA and P. L. BONORA, *Surf. Coat. Technol.* **35** (1988) 221.
9. K. OSOZAWA and N. OKATO, "Passivity and its Breakdown on Iron and Iron Based Alloys," (NACE, Houston, TX, 1976) p. 135.
10. J. E. TRUMAN, M. J. COLEMAN and K. R. PIRT, *Brit. Corros. J.* **12** (1977) 236.
11. Y. C. LU, R. BANDAY, C. R. CLAYTON and R. C. NEWMAN, *J. Electrochem. Soc.* **130** (1983) 1774.
12. U. KAMACHI MUDALI, R. K. DAYAL, T. P. S. GILL and J. B. GNANAMOORTHY, *Werkst. Korros.* **37** (1986) 637.
13. R. C. NEWMAN and T. SHAHRABI, *Corros. Sci.* **27** (1987) 827.
14. H. C. F. ROZENDAAL, P. F. COLIJN and E. J. MITTEMEIJER, *Surf. Eng.* **1** (1985) 30.
15. R. BENEKE and R. F. SANDENBERGH, *Corros. Sci.* **29** (1989) 543.
16. S. D. CHYOU and H. C. SHIH, *Mater. Sci. Eng.* **A129** (1990) 109.
17. *Idem*., *Corrosion* **47** (1991) 31.
18. M. R. NAIR, S. VENKATRAMAN, D. C. KOTHARI, K. B. LAI and R. RAMAN, *Nucl.Instrum. Methods B* **34** (1988) 53.
19. M. E. CHABICA, D. L. WILLIAMSON, R. WEI and P. J. WILBUR, *Surf. Coat. Technol.* **51** (1992) 24.
20. O. T. INAL and C. V. ROBIN, *Thin Solid Films* **95** (1982) 195.
21. S. MRIDHA and D. H. JACK, *Met. Sci.* **16** (1982) 398.
22. O. KUBASCHEWSKI and C. B. ALCOCK, "Metallurgical Thermochemistry," (Pergamon, London, 1979).
23. B. BILLON and A. HENDRY, *Surf. Eng.* **1** (1985) 114.
24. J. P. LEBRUN, H. MICHEL and M. GENTOIS, *Mem. Sci. Rev. Metall.* **69** (1972) 727.
25. E. J. MITTEMEIJER, A. B. P. VOGELS and P. J. VAN DER SCHAFF, *J. Mater. Sci.* **5** (1981) 3129.
26. V. S. AGARWALA, K. Y. KIM and S. BHATTACHARYYA, "Materials Evaluation Under Fretting Conditions," ASTM STP 780 (ASTM, Philadelphia, 1982) p. 106.
27. S. M. EL-RAHGY, H. ABD-EL-KADER and M. E. ABOU-EL-HASSAN, *Corrosion* **40** (1984) 60.
28. Y. C. LU, J. L. LUO and M. B. IVES, *ibid*. **47** (1991) 835.
29. R. J. BRISION and R. A. CAMPBELL, *Trans. ASME/AIME* **245** (1973) 239.
30. F. H. STOTT, J. E. BREAKELL and R. C. NEWMAN, *Corros. Sci.* **30** (1990) 813.
31. H. ADB-EL-KADER and S. M. EL-RAGHY, *ibid.* **26**(8) (1986) 647.
32. M. G. FONTANA and N. D. GREENE, "Corrosion Engineering," 3rd ed. (McGraw-Hill, New York, 1986), p. 73.
33. J. POSTLEHWAITE and N. W. HAWRYLAK, *Corrosion*, **31** (1975) 237.

Received 12 March 1997
and accepted 2 November 1999